Current Opinion in Solid State and Materials Science 20 (2016) 352–360

Contents lists available at ScienceDirect

Current Opinion in Solid State and Materials Science

journal homepage: www.elsevier.com/locate/cossms

Semiconductor quantum dots

Weidong Zhou [a], James J. Coleman [b,*]

[a] University of Texas at Arlington, Department of Electrical Engineering, Arlington, TX 76019, United States
[b] University of Texas at Dallas, Department of Electrical Engineering, Richardson, TX 75080, United States

ARTICLE INFO

Article history:
Received 21 January 2016
Revised 15 June 2016
Accepted 19 June 2016
Available online 7 July 2016

Keywords:
Quantum dots
Lasers
Silicon photonics
Single photon sources
Biophotonics
Solar cells

ABSTRACT

Three-dimensionally confined semiconductor quantum dots have emerged to be a versatile material system with unique physical properties for a wide range of device applications. With the advances in nanotechnology and material growth techniques for both epitaxial and colloidal quantum dots, recently the research has been shifted largely towards quantum dot based devices for practical applications. In this short review, we have tried to assemble a selection of recent advances in the areas of quantum dots for computing and communications, solid state lighting, photovoltaics, and biomedical applications that highlight the state of the art.

1. Introduction

The introduction and development of quantum wells in the 1970's had a rapid and profound impact on compound semiconductor materials and, in particular, diode lasers. In retrospect, it seems obvious that the extension of such one-dimensional quantization (wells) to two-dimensional (wires) and three-dimensional (dots) quantization should have a similar large impact. These are predicted [1–3] to introduce new physical phenomena to diode lasers and other photonic devices. In contrast to quantum wells, however, the synthesis of wire and dot structures is not straightforward. Precision growth of quantum wells in the direction normal to the growth plane in lattice-matched or lightly mismatched heterostructure systems can be obtained fairly easily with modern MOCVD and MBE growth apparatus. Quantum wires and dots require this precision as well but further require some well-controlled process that allows similar precision in one- or two-dimensions in the growth plane. The development of structures, with a suitably high density, or multiple layers, of uniform dots was the primary emphasis in research and development of these structures through the first decade of the 21st century. This has been accomplished using a variety of different approaches including growth on vicinal substrates [4], lithographically patterned structures for etching [5] or selective area epitaxy [6,7], self-assembly for strained layer materials systems [8], colloidal quantum dot solutions [9] and combinations of these [10]. There has also been, of course, incorporation of these various kinds of quantum dots into laser diodes and other, often photonic device structures. Certainly there has also been wide-ranging consideration of the quantum dot materials of choice, including elemental (column IV) semiconductors along with the, perhaps best-studied, III–V compound semiconductors.

In this short review, our goal is to highlight recent advances, particularly in the context of the likely applications for these advances. We address four distinct areas of application. The first is quantum dot lasers for computing and communications, including quantum dot lasers on silicon, quantum dot lasers with extended spectral coverage, and quantum dot lasers for single-photon sources. The second application is quantum dots for solid state lighting. The third is quantum dot solar cells with various approaches to obtaining increased quantum efficiency by means of intermediate band (IB) or multi-exciton generation (MEG) processes. Finally, we consider quantum dots for biomedical applications.

2. Quantum dot lasers for computing and communications

The three-dimensional carrier confinement and localized/discrete carrier states in QDs results in higher efficiency and differential gain with lower threshold current density and high modulation speed in QD lasers. Additionally, linewidth enhancement factor (α-factor), as well as chirp in QD lasers can be much smaller than that in QW lasers, due to a more symmetric gain function in QDs,

* Corresponding author.
E-mail address: james.coleman@utdallas.edu (J.J. Coleman).

http://dx.doi.org/10.1016/j.cossms.2016.06.006
1359-0286/

which is also critically important for high speed high performance lasers for optical communications. Finally drastically suppressed thermal spreading of the injected carriers and the relatively large energy separation between the subband levels (ground state and excited states) result in very weak temperature dependence of QD lasing threshold and large characteristic temperatures (T_0). This can lead to athermal operations of QD lasers over a wide temperature ranges [11]. It is also worth mentioning the possibility for fast dynamic response is limited by the strong damping in QD lasers. The comparably low modulation bandwidth of QD lasers is often attributed to the slow charge carrier capture into the QDs, acting as a bottleneck for the laser dynamics. Such limitations are being investigated in more details by a few groups, who proposed enhanced dynamic performance of QD lasers with scattering carrier lifetime engineering [12,13]. Several excellent reviews on QD lasers and related devices and physics were given by several groups [12,14,15]. The growth and QD size non-uniformity control for reduced inhomogeneous linewidth broadening has also been reviewed by Pelucchi et al. [16] Here we will highlight a few major advances of QD lasers for computing and communication systems.

2.1. QD lasers on silicon substrates

One of the roadblocks in silicon (Si) photonics is the reliable and practical light sources on Si substrates. Among various approaches, monolithic or hybrid integration of compound semiconductor materials on Si holds much attention due to its promising towards high performance light sources on Si. Owing to its intrinsic spectral and temperature properties, III–V QD structures are very attractive for Si photonics with potentials of large spectral coverage and uncooled high temperature operation. Impressive lasers with high output power and high operation temperature have been demonstrated by heterogeneous integration of III–V QD lasers on Si substrates through wafer bonding technique [17,18]. Such hybrid approach has led to a wide range of on-chip laser demonstrations based on different types of III–V semiconductor materials, with potentials for wafer reclamation when using smart cut or highly selective etching to perform substrate removal process [19–23].

Monolithic integration is another approach for the integration of III–V compound semiconductors on Si. However the significant material mismatch in both lattice constants and thermal expansion coefficient lead to high density dislocation and other defects generation in the III–V materials. Due to strain engineering and 3D carrier confinement, QDs have good tolerance to defects. Therefore, self-assembled QDs are being pursued actively by many groups since early 80's [15]. Breakthroughs were made over the last few years, with much reduced thread dislocations and high quality QD structures by exploring different types of Si substrates. By using multiple layers of self-organized InGaAs QDs as a very effective dislocation filter, Mi and Bhattacharya et al. reported $In_{0.5}Ga_{0.5}As$ quantum dot lasers with an $Al_{0.07}Ga_{0.93}As$ core waveguide on Si (1 0 0) substrates with 4° offcut towards the [1 1 1] direction [24–26]. A relatively low threshold current density of 900 A/cm^2 under pulsed bias conditions was measured. By modulation doping the laser device with 20 holes per dot, T_0 of 244 K in the temperature range 25–95 °C was achieved.

For optical interconnect and Si photonics applications, it is highly desirable to have Si transparent lasers with longer wavelengths at1.3 and 1.55 μm [28]. The first 1.3 μm QD laser directly grown on Si was reported by Wang et al. [29], where an InAs/InGaAs dot-in-a-well (DWELL) laser structure was directly grown on Si substrate with the use of the optimized GaAs nucleation temperature. Using InAlAs/GaAs strained-layer-superlattice (SLS) dislocation filter layers, Tang and Liu et al. [30] reported 1.3 μm InAs/GaAs QD lasers grown on Si, with a threshold current density of 194 A/cm^2 and output power of ~77 mW. Liu and Bowers et al. [27] demonstrated record performance 1.3 μm InAs QD lasers grown on Si (Fig. 1), with output power exceeding 176 mW and lasing up to 119 °C. The laser was grown on Ge-on-Si substrate, with optimal thermal treatment of the Ge surface along with the GaAs nucleation conditions. The same group also reported high reliability operation of these lasers with over 2700 h of constant current stress at 30 °C [31].

2.2. QD lasers with extended spectral coverages

Taking advantage of the broad spectral coverage, tunable lasers with wide tuning range are also being explored by many groups [32,33]. Recently, Gao et al. [34] reported broadband tunable external cavity lasers based on InAs/InP QDs grown on InP substrates, with a tuning range over 140 nm at 1550 nm spectral band with a maximum output power of 6 mW (Fig. 2).

Another area of focused research in QD lasers is to extend spectral coverage with different material systems. As discussed earlier InGaAs based QDs are largely limited to spectral range from 1 to 1.3 μm. For shorter wavelengths at visible and UV spectral regime, III-Nitride based QD structures are being investigated. As reviewed in Section 5, many interesting results have been reported over the last few years on the demonstrations of QD lasers at red, green, and blue colors.

For longer wavelengths, InP based material systems are being explored for spectral coverage towards 1.55–2 μm [14]. The growth of InAs QD grown on InP-based substrate can be easily performed the wavelength of 1.55 μm because the InAs and InP has smaller lattice mismatch (3.2%). By adjusting the size and the compound of QD on the InP substrate, the lasing spectrum can reach 2 mm. However, the growth of InAs QDs directly on (1 0 0) InP substrates typically result on reduced dot size control with stronger inhomogeneous linewidth broadening. Many research has been focused on InAs QDs grown on InP (311)B substrate, where high density QDs can be obtained owing to the high density of nucleation points for the QD islands, which also leads to the formation of more symmetric QD in the planar direction [14]. High performance lasers have been reported by a few groups over the last few years. However, challenges remain on the device process problems associated with the mis-oriented substrates, such as mirror cleaving and anisotropic etching.

Technical challenges remain in developing high performance practical and compact lasers at midwave-infrared (MWIR) wavelength range (2–5 μm), where there are important applications in gas sensing, non-invasive medical diagnosis, infrared

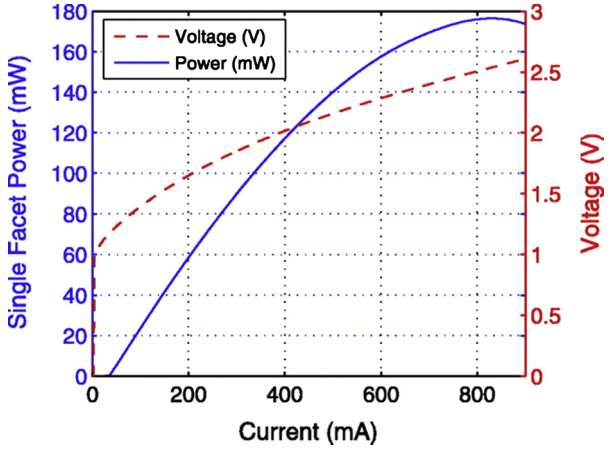

Fig. 1. LIV plot of 1.3 μm QD laser on Si. Threshold is 38 mA with 176 mW of output power at 20 °C [27].

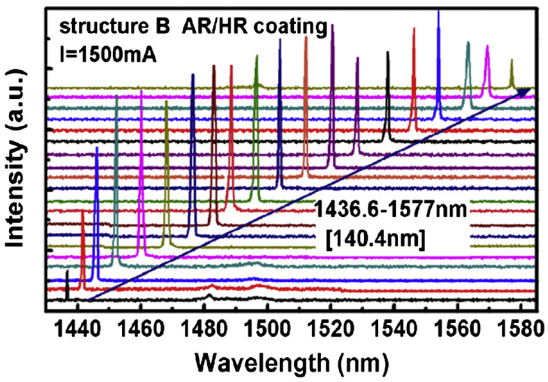

Fig. 2. Tuning spectra of 2 mm long EC InAs/InP QD gain device using structure B and AR/HR coating driven by a pulsed injection current of 1500 mA (1 kHz repetition rate and 3% duty cycle) [34].

countermeasures, and wireless communications. Owing to the unique advantages, QDs seem to be a promising gain material for high performance lasers, as compared to QWs and quantum cascade lasers. Due to the bandgap bowing effect of antimony (Sb) atoms, it is very promising to extend the emission wavelength of InAs nanostructures into MWIR by introducing some Sb atoms into InAs nanostructures to form InAsSb QDs [35]. Although, the dot density on the order of $10^{10}/cm^2$ has been achieved by several groups, t the InAsSb islands are easily elongated along [1–10] direction and form into quantum dash due to In atom mass transaction on the InAsSb layers [35]. So far, only an InAsSb QD laser grown on InP substrate with emission wavelength of 2 μm has been obtained at room temperature [36]. While, comparison with InAs QD laser, the InAsSb QD laser had a higher threshold current density of 730 A/cm^2 and poorer output power of 3 mW with a lower differential slope efficiency of 13% at temperature of 10 °C. Recently, Lu et al. [37] reported lasers around 3.1 μm based on type II In(As)Sb QD grown on (1 0 0) oriented p-InAs substrates, with operating temperature up to 120 K, and pulsed lasing threshold current densities in the order of 1.59–4.68 kA/cm^2. Much of works should be carried out on improving the performances of InAsSb QD lasers by optimizing material growth conditions for high density high quality QDs, and by improving heterostructure design for charge injection/confinement and increased modal gain.

2.3. QD lasers for single photon sources

Developing a quantum photonics network requires a source of very-high-fidelity single photons. Reducing the number of QDs to the limit of a single QD in a 3D microcavity represents the ultimate in miniaturized quantum devices [38,39]. Single QD devices play a key role for enabling the novel technology of quantum information processing, because they are the necessary deterministic sources of single and entangled photons [40–42]. Remarkable progresses have been achieved in the last decade, on demonstrations of single photon sources (SPS) with single QD in various nanophotonic cavities (e.g., see a recent review by Lodahl et al. [43]). We will highlight a few recent advances on SPSs towards practical applications.

As summarized by Lu and Pan [44], the ideal source for entangled photons (also single photons) should have the following four characteristics. (i) Deterministic generation — on a pulsed excitation, the source should emit one, and only one, pair of entangled photons with a vanishingly small chance of multi-pair emission. (ii) High fidelity — the created two-photon state should closely resemble the ideal desired entangled state. (iii) Indistinguishability —individual photons emitted in different trials should be quantum mechanically identical to each other. (iv) High collection efficiency —radiated photons should be extracted with a high efficiency so that they are not lost. Additionally, site control, room temperature operation and electrical injection are of practical importance also.

Muller et al. [45] reported the first demonstration of deterministic generation of a pair of entangled photons from a single self-assembled InAs/GaAs quantum dot. Using a clever optical pulsed two-photon resonant excitation method [46], they managed to produce, on-demand, entangled photon pairs that simultaneously have a high single-photon purity, a high entanglement fidelity and a high photon indistinguishability (Fig. 3). This result represents a large step towards fulfilling the above wish list for a photon entanglement source. However, one element from the wish list is still missing — a high photon collection efficiency. Müller et al. estimated the collection efficiency to be about 0.4%. This figure of merit needs to be substantially increased for scalable photonic quantum computing. Lu and Pan further points out this may be possible by using integrated solid immersion lenses, dielectric planar antennas [47], photonic crystal waveguides or 'photonic molecular' cavities [44]. In fact, Arcari et al. [48] reported near-unity (98.43%) coupling efficiency from a QD SPS to a photonic crystal waveguide, owing to broadband Purcell enhancement of the rate of coupling into the in-plane photonic crystal waveguide and the strong suppression of the out-of-the-plane loss rate due to the photonic crystal membrane structure.

A major drawback with commonly used III–V QDs, such as InAs QDs, for single photon devices is the need for operation at cryogenic temperatures. This difficulty can potentially be overcome by using III-nitrides and II–VI semiconductors with large bandgap offsets and improved zero dimensional confinement of carriers. Room-temperature SPS was also reported recently by Holmes et al. [49], from site-controlled III-nitride QD embedded in a nanowire (Fig. 4). The combination of using high-quality, small, site-controlled quantum dots with a wide-bandgap material system is crucial for providing both sufficient exciton confinement and an

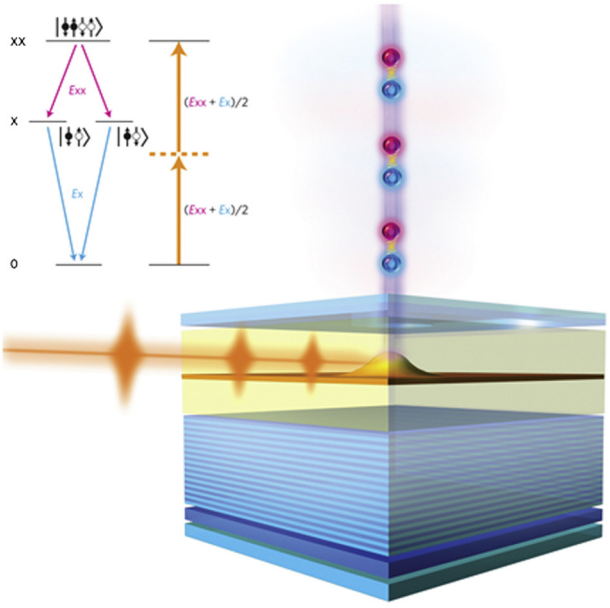

Fig. 3. The top panel shows the energy level structure of a biexciton–exciton cascade decay process. The decay starts from a biexciton (XX) state formed by two electrons and two holes. One of the electrons recombines with one of the holes and generates a first photon, leaving an exciton (X) in the dot, which subsequently also recombines to generate a second photon. The bottom panel illustrates the experimental layout; a pulsed excitation laser beam enters the semiconductor structure from the side and the emitted photon pairs are collected from the top. The single quantum dot is embedded in a planar microcavity consisting of one upper and 15 lower distributed-Bragg-reflector mirrors [44].

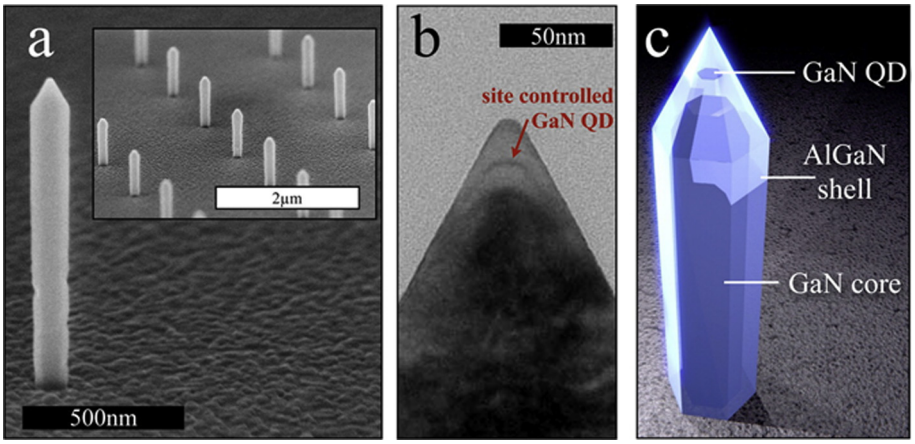

Fig. 4. Images of site-controlled nanowire-QDs. (a) SEM image showing a single nanowire grown on a patterned SiO2 substrate by selective area MOCVD. The inset shows an array of nanowires separated by 2 μm (a spacing of 20 μm was used for the optical experiments). (b) TEM image clearly showing the formation of a single QD near the tip of a single nanowire. (c) Schematic of a nanowire containing a single QD [49].

emission spectrum with minimal contamination in order to enable room temperature operation. Arrays of such single photon emitters will be useful for room-temperature quantum information processing applications such as on-chip quantum communication.

With respect to the electrical injected SPS, advances were also reported recently. Deshpande and Bhattacharya [50] reported electrically pumped single photon emission up to 150 K from a single InGaN quantum dot embedded in a GaN nanowire junction diode. The InGaN dot-in-nanowire p-n junctions were grown on silicon by molecular beam epitaxy.

In addition to epitaxial QDs, colloidal semiconductor QDs is also been investigated for SPSs owing to its simple integration schemes. Hoang et al. [51] demonstrated the regime of ultrafast spontaneous emission (~10 ps) from a single quantum emitter coupled to a plasmonic nanocavity at room temperature. The nanocavity integrated with a single colloidal semiconductor QD (CdSe/ZnS core/shell) produces a 540-fold decrease in the emission lifetime and a simultaneous 1900-fold increase in the total emission intensity. At the same time, the nanocavity acts as a highly efficient optical antenna directing the emission into a single lobe normal to the surface. This plasmonic platform is a versatile geometry into which a variety of other quantum emitters, such as crystal color centers, can be integrated for directional, room-temperature single photon emission rates exceeding 80 GHz.

With advances in SPS and single-photon detectors (SPDs), system demonstrations have been explored as well over the last few years. Takemoto et al. [52] reported long-distance quantum key distribution (QKD) by using state-of-the-art devices: a 1.5 μm band SPS and a superconducting nanowire SPD (SNSPD). They obtained the maximal secure key rate of 27.6 bps without using decoy states, which is at least threefold larger than the rate obtained in the previously reported 50-km long QKD experiment. They also succeeded in transmitting secure keys at the rate of 0.307 bps over 120 km.

3. Quantum Dots for Solid State Lighting (QD-SSL)

Solid-state lighting (SSL) has made tremendous progress in the past decade, with dramatic increase in efficiency and reduction in cost. Currently, the state-of-the-art SSL architecture is based on blue LEDs combined with green, yellow, and/or red phosphors, the so called phosphor-converted LED (PC-LED), which has an overall wall plug efficiency of 30%, considering the efficiencies for blue LED (50%), phosphor conversion and packaging (70%), and spectral match to the human eye response (85%) [53]. Further increase in efficiency in PC-LEDs may be limited by the Stokes deficit on converting from blue to green and red (25%). To achieve ultra-efficient (>70%) and smart (spectral tuning and visible light communications for internet of things) SSL, PC-LED must give way to phosphor-free multi-color semiconductor electroluminescent SSL architecture [53]. While theoretically it is possible to achieve ultra-efficient phosphor-free SSL with multi-color semiconductor electroluminescent devices (LEDs or LDs), the challenges remain in improving material qualities and in new device architectures. Currently the wall plug efficiencies for blue (460 nm), red (614 nm), and green or yellow (535 nm and 573 nm) are 50%, 30%, and 20%, respectively. Mostly, the efforts have been focused on nitride-based materials and nanostructures for SSL with higher efficiencies.

QDs, owning to its unique features of size dependent emission spectral properties, and excellent temperature independent operation, offer an excellent solution. Compared to QW based LEDs, III-Nitride QDs offer superior three-dimensional carrier confinement and drastically reduced dislocation densities and polarization fields in the device active region, with enhanced internal quantum efficiency. One of the interesting structures investigated by Mi and co-workers [54] is a full-color InGaN/GaN dot-in-a-wire LED structure, grown on n-type Si (1 1 1) substrates using MBE system under nitrogen-rich conditions (Fig. 5). By controlling the indium content in the QDs in a single epitaxial growth step, the authors demonstrated phosphor-free white LEDs with >20% internal quantum efficiency and no apparent "efficiency droop" was observed for current densities up to ~200 A/cm^2.

"Efficiency droop" refers to the reduction in efficiency as the input current density increases. It is one of challenges limiting LED based SSL efficiencies, especially at higher injection current densitites. The droop phenomenon occurs primarily by a mechanism of non-radiative Auger recombination. However, Auger recombination at higher currents in III-nitride LEDs cannot grow (is clamped) in LDs after threshold [55,56]. Therefore, substituting LDs for LEDs as a SSL source is a method to circumvent efficiency droop. This could enable high flux emitter with high efficiencies at higher current densities.

Semiconductor lasers at visible wavelengths have been developed mostly based on InGaN/GaN QW heterostructures grown on c-plane polar GaN substrates. It is known that the polarization fields in the QWs are very large when grown on the c-plane. Recently laser diodes have been demonstrated on the non-polar GaN planes which have reduced polarization field as compared

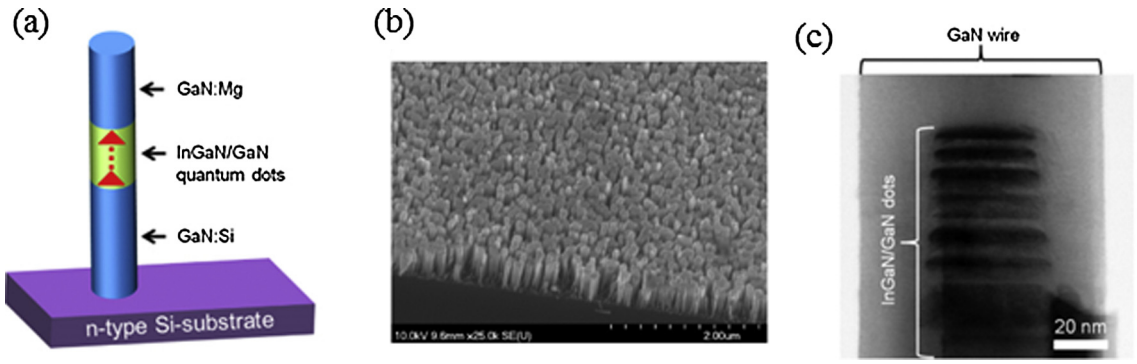

Fig. 5. Nitride QD in a wire: (a) Schematic illustration of the dot-in-a-wire LED heterostructure on silicon; (b) A 45° tilted scanning electron microscopy image of the InGaN/GaN dot-in-a-wire heterostructures grown on a Si (1 1 1) substrate by molecular beam epitaxy; (c) STEM image of the active region of an InGaN/GaN dot-in-a-wire LED heterostructure [54].

with the c-plane QW laser structures. However difficulties in incorporating indium in the InGaN/GaN QWs on these substrates impede the growth and performance of such lasers. As an alternative, devices which make use of InGaN/GaN QDs in the active region have several advantages such as increased carrier confinement, smaller piezoelectric field, reduced quantum confined Stark effect and blue-shift in emission wavelength, reduced carrier lifetimes. Blue-, green-, and very recently, red-emitting LDs have been reported by Bhattacharya and co-workers [57–61], based on InGaN/GaN QDs grown by MBE on GaN/sapphire substrate. The demonstrated devices have internal quantum efficiencies of 35–40%. Further improvement in material quality (Dislocations and other defects) may lead to much improved efficiencies. Another advantage of these QD LDs is the large characteristic temperature (To = 236 K) [62], which can lead to high efficient high power operations at even higher temperatures.

While QD holds great promises in addressing some of the challenging issues facing future SSL in smart and ultra-efficient SSL, issues remain in materials growth, device architecture, and packaging. Dot size uniformity and density control remains to be an area of material challenge. For wide spread of cost effective SSL, QDs grown on low cost substrates with very low defect density and high performance is of great interest. While QD laser based SSLs may offer advantages with higher energy efficiency at higher injection currents, threshold reduction with improved material qualities and innovations device structures are needed, including reductions in non-radiative recombination and increase in spontaneous emission factors.

Another critical issue in nitride based light sources is the difficulties in p-type doping for efficient hole injection and transport processes in InGaN/GaN nanoscale heterostructures, caused by the heavy effective mass, small mobility, and low concentration of holes. One of the interesting approaches is the use of p-type modulation doping in the quantum dot active region, reported by Mi and co-workers [63]. They demonstrated phosphor-free white LEDs with a record high (~56.8%) internal quantum efficiency, which is attributed to the superior carrier confinement provided by the dots and the significantly enhanced hole transport, due to the p-type modulation doping.

In addition to the epitaxial QDs, chemically synthesized colloidal QDs (CQDs) also attracted great attention due to its wide spectral coverage, size-dependent tenability, and potentially low cost material preparation and fabrication processes [64]. However, due to the complications in surface control and charge injection, overall energy efficiency of CQD LEDs is still much lower than epitaxial QD based LEDs, and even lower than organic LEDs [65,66]. To date, the reported maximum external quantum efficiencies are 7.1%, 12.6%, and 18–20% for deep-blue, green, and red CQD-LEDs, based on different CQD synthesis procedures and different device architectures [67–69]. For white light SSL and display applications, it is also highly desirable to have a common device structure to achieve high efficiencies for all three colors. Recently, Yang et al. [65] reported a full series of blue, green and red CQD-LEDs with external quantum efficiencies of 10.7%, 14.5%, and 12%, made using the same solution processed device structures, with fine control of the composition of the graded intermediate shell and the thickness of the outer shell, in a core-shell CQD configuration.

Major challenges related to CQD-LEDs are surface control for reduced non-radiative recombination (Surface and Auger), efficient charge injection, most importantly thermal and photoquenching [70], where the quantum yields tend to decrease, sometimes permanently, when exposed to high temperatures and photo fluxes.

4. Quantum Dot Solar Cells (QDSCs)

Quantum dot solar cells (QDSCs) can potentially surpass the Shockley Queisser limit for single-junction solar cell efficiency owing to various mechanisms for parallel photovoltaic (PV) conversion of wide band solar spectrum [71]. In addition to the absorption of photons with energy great than bandgaps, sub-bandgap absorption is feasible via the intermediate band (IB, or subbands) in QDs to generate an additional photocurrent from low energy photons of the solar spectrum [72,73]. While the above-bandgap high energy photons are wasted in conventional semiconductors due to fast thermalization of hot photoelectrons, it may be converted in QD media via multiple exciton generation [74] and via thermionic emission from QDs induced by hot photoelectrons [75].

Significant efforts in optimization of conversion processes were concentrated at the intermediate band solar cell (IBSC) QD materials [15]. Luque and Marti [76] calculated a theoretical efficiency of 63%, well exceeding the Shockley-Queisser model efficiency, from an ideal single junction IBSC. To obtain the highest theoretical efficiencies for IBSCs, a high bandgap of 1.93 eV is required with sub-bandgaps of 0.7 eV and 1.2 eV under "maximum concentration" [76]. Therefore the conversional InAs/GaAs QD system is not an ideal candidate for IBSCs. In order to enhance quantum confinement, attempts using high bandgap materials, such as InAlGaAs, AlAs, AlGaAs, and InGaP to host In(Ga)As QDs have shown reasonable successes [77]. Sablon et al. [71] proposed an approach to optimization of QDSC materials based on engineering of potential profile in QD media with localized intermediate states, which are controllably filled by selective doping of the interdot regions. Effects of concentrated solar radiation on PV performance were investigated by Sablon et al. [71] in such well-developed GaAs

QDSCs with one-sun efficiencies of 18–19%. They also predicted efficiencies greater than 24% at thousand Suns are feasible by the additional improvement in front-contact resistance.

Challenges remain in strain engineering and material growth optimization with the choice of different barrier and wetting layers for longer lifetime of the charge carriers in QDs, and for the control of thermal coupling and optimum QD confinement potentials.

Multi-exciton generation (MEG) was also investigated extensively, though mostly on colloidal QD (CQD) material systems [78,79]. MEG occurs in semiconductors when excitons with energy greater than twice the band gap energy relax to the band edge by exciting an additional electron-hole pair (EHP) through impact ionization [80]. In an ideal MEG solar cell, EQE would exceed 100% for energies greater than twice the ban gap energy because high energy photons could produce more than one EHP. Again, if a threshold of twice the band gap energy could be realized for impact ionization in a CQD solar cell, the theoretical maximum power conversion efficiency would shift to above 60% [74].

Heteroepitaxy is another direction towards multi-junction solar cells, where different crystalline materials are formed in epitaxial process, mostly based on vacuum based MBE or MOCVD techniques. Recently, heteroepitaxy of QD in perovskite solids were reported by Ning et al. [81] where crystalline coherence is preserved even when the atomic identity is modulated (Fig. 6). Potentials in bulk organohalide semiconductor perovskites have led to advances in materials and improved performance in perovskite solar cells. Ning et al. [81] reported remarkable optoelctronic properties in the heterocrystals that are traceable to their atom-scale crystalline coherence: photoelectrons and holes generated in the larger-bandgap perovskites are transferred with 80% efficiency to become excitons in CQDs. This can be an interesting solution based platform for low cost high performance optoelectronic devices and solar cells.

5. Quantum dots for biomedical applications

Semiconductor QDs, mostly colloidal QDs, are widely investigated for biomedical applications in labeling, imaging, targeted-drug delivery, sensing, and therapy. There are a few excellent comprehensive reviews recently on this subject [82–84]. Here we highlight a few major research advances.

The synthesis of CQDs has been mostly focused on the biocompatibility and low-toxicity. Typically, as-synthesized CQDs are capped with hydrophobic molecules and need to be solubilized in aqueous solution before practical use. The solubilization step can be achieved by either ligand exchange or encapsulation of QDs with amphipathic polymers, or further decorated by water-soluble silica shells [83]. Subsequently the QDs can be conjugated with biomolecules for specific labeling or targeting, which could be achieved by covalent bioconjugation chemistry, biotin-avidin interaction, electrostatic interaction etc. Recently as an alternative approach, aqueous solution-based synthesis has attracted more attentions due to its mild synthetic conditions, the elimination of the solubilization step, and the use of simple and cheap reaction instruments. One of the most interesting directions is to synthesize CQDs in living organisms. Living cells such as yeast and *E. coli* cells could serve as reactors to mediate the formation of QDs following the introduction of QD precursors into the cells (Fig. 7) [85,86]. The intracellular glutathione molecules or the genetically encoded QD binding peptide could serve as ligands to mediate the formation of the QDs in the cells. In fact, the QD can be synthesized even in whole living organisms, such as the recent reports of CdTe QD synthesis in earthworm [87]. Another issue to be considered in CQD synthesis is the toxicity [88]. Heavy metals used in these CQD raised some concern about its impact if left inside the body. While small QDs with sizes less than 5 nm can be removed from kidney, CQDs with larger sizes is another concern.

Janus particle (JP) is another type of surface functionalized QDs, which attracted great attention recently [89,90]. It refers to colloid-sized particles with two regions of different surface chemical composition with broken symmetry. While the huge majority of synthetic building blocks has (centro)symmetric morphology and interaction potentials (e.g., Coulomb interaction), this is rarely found in natural systems. Therefore, the introduction of complexity through asymmetry is a major challenge in synthetic nanochemistry (Fig. 8). Hetero-nanoparticles facilitate an even more advanced approach toward the design of today's highly desired multifunctional nanoparticles used in research at the interface between materials science, biotechnology, and medicine. Hetero-nanoparticles enable access to widespread technological scenarios. These hybrid materials represent artificial platforms generating synergistically enhanced, tunable chemical and physical characteristics, or even cause the emergence of phenomena, which would not be accessible using homogeneous nanomaterials. Recent developments in the fields of hetero-structured QDs are the formation of anisotropic, namely elongated structures, whereby the variation of the aspect ratio allows control of the electron–hole overlap [89].

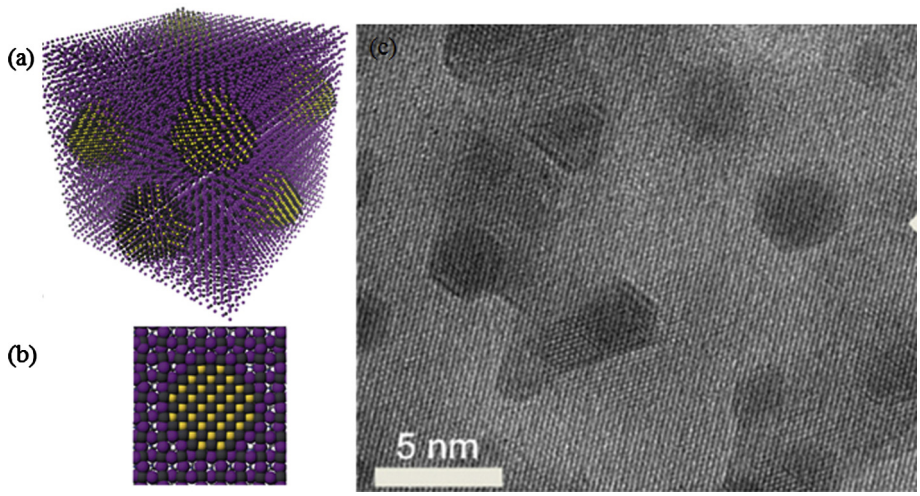

Fig. 6. Quantum-dot-in-perovskite solids: (a) Theoretical three-dimensional atomistic model of CQDs in a perovskite matrix; (b) Cross-section (two-dimensional view) of a single CQD in perovskite; and (c) A TEM image of CQD–perovskite hybrid [81].

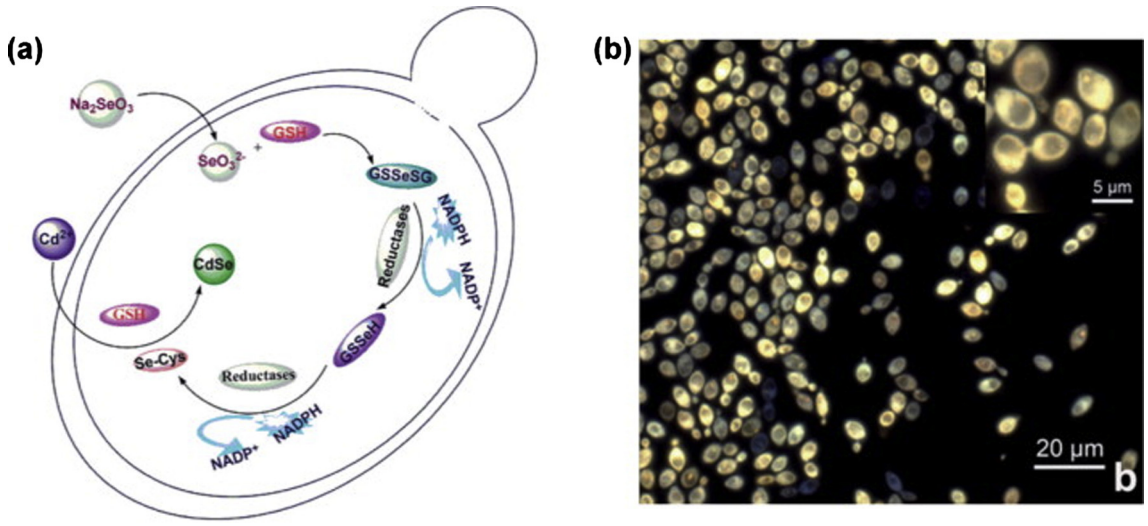

Fig. 7. Synthesis of QDs in yeast cells. (a) Route for unnatural biosynthesis of fluorescent CdSe quantum dots and (b) images for subcellular location of intracellular fluorescence [83].

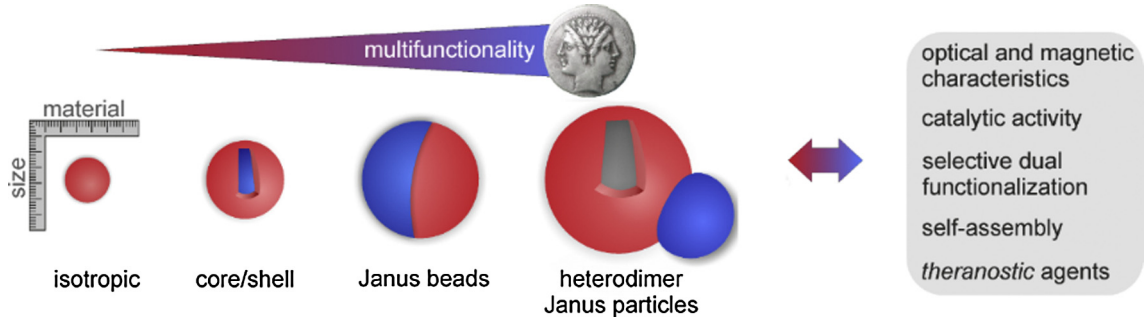

Fig. 8. Illustrations of the transition from isotropic to anisotropic particles [89].

This leads to an exceptional size-dependent quantum Stark effect due to the increased spatial volume enabling effective charge carrier separation [20]. The design of anisotropically shaped semiconductors is limited since the band-edge luminescence is further reduced due to a higher surface-to-volume ratio and the increased carrier delocalization lowering the probability of a radiative carrier recombination [10]. But their major drawback, the uniformity of the surface, remains. Janus particles are outstanding among the hetero-nanoparticles owing to their asymmetry as an additional design module. Therefore, they are able to combine even very different chemical and physical properties within a single particle.

Based upon the combination of optical, magnetic, and catalytic properties within one nanoparticle, inorganic hybrid materials have attracted increasing attention owing to their easily tunable properties by variation of materials, domain sizes, and morphology. Aside from the properties of the single components added one by one to form the properties of the heterostructure, several new properties emerge from the morphology and surface chemistry of the heterodimers. Chen and co-workers [91] introduced JPs with superparamagnetic NPs confined in one black hemisphere and quantum dots (QDs) localized in the other white/fluorescent hemisphere (Fig. 9(a)). The bifunctional magnetic-fluorescent Janus beads were employed to fabricate a magnetically switchable display, operating both in optical reflection and in fluorescence mode, in which individual JPs served as singular pixels.

Another area of applications for hetero-structured JP particles is in the rapid and sensitive detection of pathogens, for specific cell labeling, in vitro and in vivo imaging, or for the targeted delivery and on demand release of pharmaceuticals in site-specific treatments of injuries or diseases. Undoubtedly, these developments are en route to revolutionizing bio-sensing and bioseparation technology and pave the ways for unprecedented ways of disease detection and curing. Progress in the direction of higher control and precision in selective targeting, sensing, and release depends heavily on better ways to produce more complex and multifunctional particles. Consequently, considering that JPs can combine various inorganic and (bio)organic functionalities on different hemispheres with possibly vastly different physical and biochemical properties, significant promise arises from using them for applications interfacing the biological world.

One of the possibilities certainly lies in the option to spatially separate nanoscale biodetection/sensing from external manipulation or macroscopic detection in a way that either methods or chemical groups may not interfere. Various groups reported on strategies targeting this issue. For instance, Lahann's group [92] used polymer-based Janus spheres, prepared via electrohydrodynamic co-jetting, with one side modified with biotin tags and each side additionally labeled with green and red (HUVECs, or Human umbilical vein endothelialcells) (Fig. 9(b)). A control experiment to a biotinisotype antibody revealed no association between the HUVEC cells and the beads. The presence of an additional homogeneous polyethylene glycol (PEG) coating on the Janus beads assisted in suppressing any non-specific adhesion. Notably, a high biocompatibility was found as the presence of non-binding particles did not affect the proliferation of the cell line in the investigated concentration and time regime.

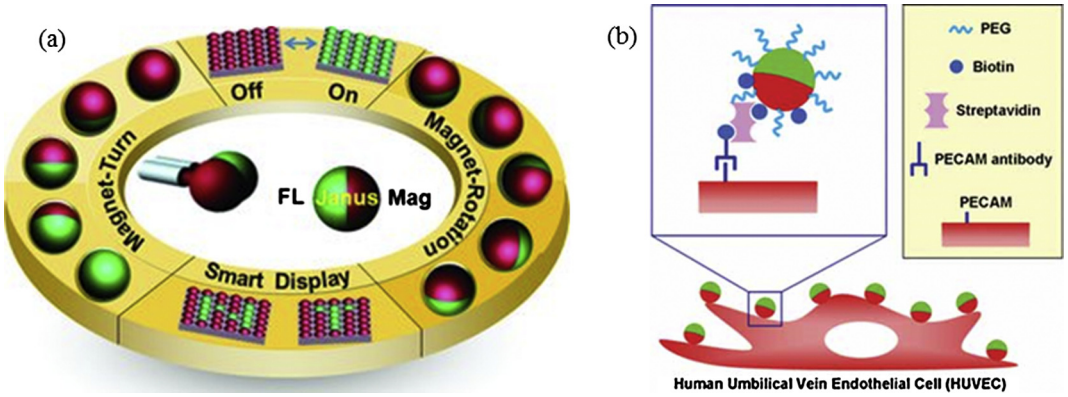

Fig. 9. Janus particle examples. (a) The first microfluidic synthesis of ionomer-based bifunctional Janus superballs possessing two distinct magnetic-nanoparticle-dropped and CdS quantum dots–polymer hemispheres within an anisotropic structure. Based on such Janus superballs with stable fluorescence and superparamagnetism, a magnetoresponsive fluorescent switch is developed to realize free-writing under a magnetic field [91]; and (b) Biocompatible anisotropic polymer particles with bipolar affinity towards human endothelial cells are a novel type of building blocks for microstructured bio-hybrid materials. Functional polarity due to two biologically distinct hemispheres has been achieved by synthesis of anisotropic particles via electro-hydrodynamic co-jetting of two different polymer solutions and subsequent selective surface modification [92].

6. Conclusions

After nearly a generation of intensive effort on developing the growth, synthesis, choice of materials and characterization of semiconductor quantum dots, development in the last few years has been defined in the context of the kinds of applications for which these structures are most appropriate. In this short review, we have tried to assemble a selection of recent advances in the areas of quantum dots for computing and communications, solid state lighting, photovoltaics, and biomedical applications that highlight the state of the art. A simple literature search on the phrase "semiconductor quantum dots" for the year 2015 alone yields more than 3700 citations. Clearly, we were only able to skim the surface in this review. It is likely that the reader could find many other examples worthy of inclusion. We apologize for any omissions.

Acknowledgements

This work was supported by the Erik Jonsson School of Engineering Distinguished Chair (JJC), by US Air Force Office of Scientific Research, and by the US Army Research Office.

References

[1] P. Blood, Quantum confined laser devices, 2015.
[2] Y. Arakawa, H. Sakaki, Multidimensional quantum well laser and temperature dependence of its threshold current, Appl. Phys. Lett. 40 (1982) 939–941.
[3] Y. Arakawa, K. Vahala, A. Yariv, Quantum noise and dynamics in quantum well and quantum wire lasers, Appl. Phys. Lett. 45 (1984) 950–952.
[4] T. Fukui, H. Saito, M. Kasu, S. Ando, MOCVD methods for fabricating GaAs quantum wires and quantum dots, J. Cryst. Growth 124 (1992) 493–496.
[5] V. Verma, J. Coleman, High density patterned quantum dot arrays fabricated by electron beam lithography and wet chemical etching, Appl. Phys. Lett. 93 (2008) 111117.
[6] R. Bhat, E. Kapon, D. Hwang, M. Koza, C. Yun, Patterned quantum well heterostructures grown by OMCVD on non-planar substrates: Applications to extremely narrow SQW lasers, J. Cryst. Growth 93 (1988) 850–856.
[7] T.S. Yeoh, R.B. Swint, A. Gaur, V.C. Elarde, J. Coleman, Selective growth of InAs quantum dots by metalorganic chemical vapor deposition, IEEE J. Select. Top. Quant. Electron. 8 (2002) 833–838.
[8] P. Petroff, S. DenBaars, MBE and MOCVD growth and properties of self-assembling quantum dot arrays in III-V semiconductor structures, Superlattice Microst. 15 (1994) 15.
[9] T. Rajh, O.I. Micic, A.J. Nozik, Synthesis and characterization of surface-modified colloidal cadmium telluride quantum dots, J. Phys. Chem. 97 (1993) 11999–12003.
[10] N. Dias, A. Garg, U. Reddy, J. Young, V. Verma, R. Mirin, et al., Directed self-assembly of InAs quantum dots on nano-oxide templates, Appl. Phys. Lett. 98 (2011) 141112.
[11] Y. Urino, N. Hatori, K. Mizutani, T. Usuki, J. Fujikata, K. Yamada, et al., First demonstration of athermal silicon optical interposers with quantum dot lasers operating up to 125 °C, J. Lightwave Technol. 33 (2015) 1223–1229.
[12] W.W. Chow, F. Jahnke, On the physics of semiconductor quantum dots for applications in lasers and quantum optics, Prog. Quant. Electron. 37 (2013) 109–184.
[13] C. Wang, B. Lingnau, K. Ludge, J. Even, F. Grillot, Enhanced dynamic performance of quantum dot semiconductor lasers operating on the excited state, IEEE J. Quant. Electron. 50 (2014) 723–731.
[14] S.G. Li, Q. Gong, C.F. Cao, X.Z. Wang, J.Y. Yan, Y. Wang, et al., The developments of InP-based quantum dot lasers, Infrared Phys. Technol. 60 (2013) 216–224.
[15] J. Wu, S. Chen, A. Seeds, H. Liu, Quantum dot optoelectronic devices: lasers, photodetectors and solar cells, J. Phys. D 48 (2015) 363001.
[16] E. Pelucchi, V. Dimastrodonato, L. Mereni, G. Juska, A. Gocalinska, Semiconductor nanostructures engineering: pyramidal quantum dots, Curr. Opin. Solid State Mater. Sci. 16 (2012) 45–51.
[17] K. Tanabe, D. Guimard, D. Bordel, S. Iwamoto, Y. Arakawa, Electrically pumped 1.3 μm room-temperature InAs/GaAs quantum dot lasers on Si substrates by metal-mediated wafer bonding and layer transfer, Opt. Express 18 (2010) 10604–10608.
[18] S. Tanaka, S.-H. Jeong, S. Sekiguchi, T. Kurahashi, Y. Tanaka, K. Morito, High-output-power, single-wavelength silicon hybrid laser using precise flip-chip bonding technology, Opt. Express 20 (2012) 28057–28069.
[19] D. Liang, J.E. Bowers, Recent progress in lasers on silicon, Nat. Photon. 4 (2010) 511–517.
[20] D. Liang, G. Roelkens, R. Baets, J.E. Bowers, Hybrid integrated platforms for silicon photonics, Materials 3 (2010) 1782–1802.
[21] H. Yang, D. Zhao, S. Chuwongin, J.-H. Seo, W. Yang, Y. Shuai, et al., Transfer-printed stacked nanomembrane lasers on silicon, Nat. Photon. 6 (2012) 617–622.
[22] W. Zhou, D. Zhao, Y.-C. Shuai, H. Yang, S. Chuwongin, A. Chadha, et al., Progress in 2D photonic crystal Fano resonance photonics, Prog. Quant. Electron. 38 (2014) 1–74.
[23] J.E. Bowers, J.T. Bovington, A.Y. Liu, A.C. Gossard, A path to 300 mm hybrid silicon photonic integrated circuits, in: Optical Fiber Communication Conference Optical Society of America, 2014.
[24] Z. Mi, P. Bhattacharya, J. Yang, K.P. Pipe, Room-Temperature Self-Organised $In_{0.5}Ga_{0.5}As$ Quantum Dot Laser on Silicon, Electron. Lett.: Institution of Engineering and Technology, 2005, pp. 742–744.
[25] Z. Mi, J. Yang, P. Bhattacharya, D. Huffaker, Self-organised quantum dots as dislocation filters: the case of GaAs-based lasers on silicon, Electron. Lett. 42 (2006) 121–123.
[26] Y. Jun, P. Bhattacharya, Z. Mi, High-performance $In_{0.5}Ga_{0.5}As$/GaAs quantum-dot lasers on silicon with multiple-layer quantum-dot dislocation filters, IEEE Trans. Electron Dev. 54 (2007) 2849–2855.
[27] A.Y. Liu, C. Zhang, J. Norman, A. Snyder, D. Lubyshev, J.M. Fastenau, et al., High performance continuous wave 1.3 μm quantum dot lasers on silicon, Appl. Phys. Lett. 104 (2014) 041104.
[28] S. Chen, M. Tang, J. Wu, Q. Jiang, V. Dorogan, M. Benamara, et al., Long-Wavelength InAs/GaAs Quantum-Dot Light Emitting Sources Monolithically Grown on Si Substrate, Multidisciplinary Digital Publishing Institute, Photonics, 2015, pp. 646–658.
[29] T. Wang, H. Liu, A. Lee, F. Pozzi, A. Seeds, 1.3-μm InAs/GaAs quantum-dot lasers monolithically grown on Si substrates, Opt. Express 19 (2011) 11381–11386.
[30] M. Tang, S. Chen, J. Wu, Q. Jiang, V.G. Dorogan, M. Benamara, et al., 1.3-μm InAs/GaAs quantum-dot lasers monolithically grown on Si substrates using InAlAs/GaAs dislocation filter layers, Opt. Express 22 (2014) 11528–11535.

[31] A. Liu, R. Herrick, O. Ueda, P. Petroff, A. Gossard, J. Bowers, Reliability of InAs/GaAs quantum dot lasers epitaxially grown on silicon, 2015.
[32] H. Li, G.T. Liu, P.M. Varangis, T.C. Newell, A. Stintz, B. Fuchs, et al., 150-nm tuning range in a grating-coupled external cavity quantum-dot laser, IEEE Photon. Technol. Lett. 12 (2000) 759–761.
[33] P. Chen, Q. Gong, C.F. Cao, S.G. Li, Y. Wang, Q.B. Liu, et al., High performance external cavity InAs/InP quantum dot lasers, Appl. Phys. Lett. 98 (2011) 121102.
[34] F. Gao, S. Luo, H.M. Ji, X.G. Yang, P. Liang, T. Yang, Broadband tunable InAs/InP quantum dot external-cavity laser emitting around 1.55 & #x03BC;m, Opt. Express 23 (2015) 18493–18500.
[35] W. Lei, H.H. Tan, C. Jagadish, Formation and shape control of InAsSb/InP (0 0 1) nanostructures, Appl. Phys. Lett. 95 (2009) 013108.
[36] Y. Qiu, D. Uhl, S. Keo, Room-temperature continuous-wave operation of InAsSb quantum-dot lasers near 2 μm based on (0 0 1) InP substrate, Appl. Phys. Lett. 84 (2004) 263–265.
[37] Q. Lu, Q. Zhuang, A. Krier, Gain and Threshold Current in Type II In (As) Sb Mid-Infrared Quantum Dot Lasers, Multidisciplinary Digital Publishing Institute, Photonics, 2015, pp. 414–425.
[38] J.P. Reithmaier, G. Sek, A. Loffler, C. Hofmann, S. Kuhn, S. Reitzenstein, et al., Strong coupling in a single quantum dot-semiconductor microcavity system, Nature 432 (2004) 197–200.
[39] T. Yoshie, A. Scherer, J. Hendrickson, G. Khitrova, H.M. Gibbs, G. Rupper, et al., Vacuum rabi splitting with a single quantum dot in a photonic crystal nanocavity, Nature 432 (2004) 200–203.
[40] P. Michler, A. Kiraz, C. Becher, W. Schoenfeld, P. Petroff, L. Zhang, et al., A quantum dot single-photon turnstile device, Science 290 (2000) 2282–2285.
[41] A. Mohan, M. Felici, P. Gallo, B. Dwir, A. Rudra, J. Faist, et al., Polarization-entangled photons produced with high-symmetry site-controlled quantum dots, Nat. Photon. 4 (2010) 302–306.
[42] C.L. Salter, R.M. Stevenson, I. Farrer, C.A. Nicoll, D.A. Ritchie, A.J. Shields, An entangled-light-emitting diode, Nature 465 (2010) 594–597.
[43] P. Lodahl, S. Mahmoodian, S. Stobbe, Interfacing single photons and single quantum dots with photonic nanostructures, Rev. Mod. Phys. 87 (2015) 347–400.
[44] C.-Y. Lu, J.-W. Pan, Quantum optics: push-button photon entanglement, Nat. Photon. 8 (2014) 174–176.
[45] M. Muller, S. Bounouar, K.D. Jons, M. Glassl, P. Michler, On-demand generation of indistinguishable polarization-entangled photon pairs, Nat. Photon. 8 (2014) 224–228.
[46] H. Jayakumar, A. Predojević, T. Huber, T. Kauten, G.S. Solomon, G. Weihs, Deterministic photon pairs and coherent optical control of a single quantum dot, Phys. Rev. Lett. 110 (2013) 135505.
[47] J.-M. Gerard, J. Claudon, J. Bleuse, M. Munsch, N. Gregersen, Very efficient single-photon sources based on quantum dots in photonic wires, in: 2014 International on Semiconductor Laser Conference (ISLC), IEEE, 2014, pp. 1–2.
[48] M. Arcari, I. Söllner, A. Javadi, S. Lindskov Hansen, S. Mahmoodian, J. Liu, et al., Near-unity coupling efficiency of a quantum emitter to a photonic crystal waveguide, Phys. Rev. Lett. 113 (2014) 093603.
[49] M.J. Holmes, K. Choi, S. Kako, M. Arita, Y. Arakawa, Room-temperature triggered single photon emission from a III-nitride site-controlled nanowire quantum dot, Nano Lett. 14 (2014) 982–986.
[50] S. Deshpande, P. Bhattacharya, An electrically driven quantum dot-in-nanowire visible single photon source operating up to 150 K, Appl. Phys. Lett. 103 (2013) 241117.
[51] T.B. Hoang, G.M. Akselrod, M.H. Mikkelsen, Ultrafast room-temperature single photon emission from quantum dots coupled to plasmonic nanocavities, Nano Lett. (2015).
[52] K. Takemoto, Y. Nambu, T. Miyazawa, Y. Sakuma, T. Yamamoto, S. Yorozu, et al., Quantum key distribution over 120 km using ultrahigh purity single-photon source and superconducting single-photon detectors, Sci. Rep. 5 (2015) 14383.
[53] J.Y. Tsao, M.H. Crawford, M.E. Coltrin, A.J. Fischer, D.D. Koleske, G.S. Subramania, et al., Toward smart and ultra-efficient solid-state lighting, Adv. Opt. Mater. 2 (2014) 809–836.
[54] H.P.T. Nguyen, K. Cui, S. Zhang, S. Fathololoumi, Z. Mi, Full-color InGaN/GaN dot-in-a-wire light emitting diodes on silicon, Nanotechnology 22 (2011) 445202.
[55] J.J. Wierer, J.Y. Tsao, Advantages of III-nitride laser diodes in solid-state lighting, Phys. Status Solidi A 212 (2015) 980–985.
[56] L.Y. Kuritzky, J.S. Speck, Lighting for the 21st century with laser diodes based on non-basal plane orientations of GaN, MRS Commun. 5 (2015) 463–473.
[57] A. Banerjee, T. Frost, E. Stark, P. Bhattacharya, Continuous-wave operation and differential gain of InGaN/GaN quantum dot ridge waveguide lasers (λ = 420 nm) on c-plane GaN substrate, Appl. Phys. Lett. 101 (2012) 041108.
[58] M. Zhang, A. Banerjee, C.-S. Lee, J.M. Hinckley, P. Bhattacharya, A InGaN/GaN quantum dot green (λ = 524 nm) laser, Appl. Phys. Lett. 98 (2011) 221104.
[59] T. Frost, A. Banerjee, K. Sun, S.L. Chuang, P. Bhattacharya, InGaN/GaN quantum dot red (λ = 630 nm) laser, 2013.
[60] A. Banerjee, T. Frost, P. Bhattacharya, Nitride-based quantum dot visible lasers, J. Phys. D 46 (2013) 264004.
[61] T. Frost, A. Banerjee, P. Bhattacharya, Small-signal modulation and differential gain of red-emitting (λ = 630 nm) InGaN/GaN quantum dot lasers, Appl. Phys. Lett. 103 (2013) 211111.
[62] T. Frost, A. Banerjee, K. Sun, S.L. Chuang, P. Bhattacharya, InGaN/GaN quantum dot red laser, IEEE J. Quant. Electron. 49 (2013) 923–931.
[63] H.P.T. Nguyen, S. Zhang, K. Cui, X. Han, S. Fathololoumi, M. Couillard, et al., P-Type modulation doped InGaN/GaN dot-in-a-wire white-light-emitting diodes monolithically grown on Si (1 1 1), Nano Lett. 11 (2011) 1919–1924.
[64] A.P. Alivisatos, Semiconductor clusters, nanocrystals, and quantum dots, Science 271 (1996) 933–937.
[65] Z. Yang, O. Voznyy, M. Liu, M. Yuan, A.H. Ip, O.S. Ahmed, et al., All-Quantum-dot infrared light-emitting diodes, ACS Nano (2015).
[66] N. Thejokalyani, S. Dhoble, Novel approaches for energy efficient solid state lighting by RGB organic light emitting diodes–a review, Renew. Sustain. Energy Rev. 32 (2014) 448–467.
[67] K.-H. Lee, J.-H. Lee, W.-S. Song, H. Ko, C. Lee, J.-H. Lee, et al., Highly efficient, color-pure, color-stable blue quantum dot light-emitting devices, ACS Nano 7 (2013) 7295–7302.
[68] K.-H. Lee, J.-H. Lee, H.-D. Kang, B. Park, Y. Kwon, H. Ko, et al., Over 40 cd/a efficient green quantum dot electroluminescent device comprising uniquely large-sized quantum dots, ACS Nano 8 (2014) 4893–4901.
[69] B.S. Mashford, M. Stevenson, Z. Popovic, C. Hamilton, Z. Zhou, C. Breen, et al., High-efficiency quantum-dot light-emitting devices with enhanced charge injection, Nat. Photon. 7 (2013) 407–412.
[70] M.E. Coltrin, A.M. Armstrong, I. Brener, W.W. Chow, M.H. Crawford, A.J. Fischer, et al., Energy Frontier research center for solid-state lighting science: exploring new materials architectures and light emission phenomena, J. Phys. Chem. C 118 (2014) 13330–13345.
[71] K. Sablon, Y. Li, N. Vagidov, V. Mitin, J. Little, H. Hier, et al., GaAs quantum dot solar cell under concentrated radiation, Appl. Phys. Lett. 107 (2015) 073901.
[72] M.C. Beard, J.M. Luther, A.J. Nozik, The promise and challenge of nanostructured solar cells, Nat. Nanotechnol. 9 (2014) 951–954.
[73] R. Tamaki, Y. Shoji, Y. Okada, K. Miyano, Spectrally resolved intraband transitions on two-step photon absorption in InGaAs/GaAs quantum dot solar cell, Appl. Phys. Lett. 105 (2014) 073118.
[74] R.D. Schaller, V.I. Klimov, High efficiency carrier multiplication in PbSe nanocrystals: implications for solar energy conversion, Phys. Rev. Lett. 92 (2004) 186601.
[75] K. Sablon, J. Little, N. Vagidov, Y. Li, V. Mitin, A. Sergeev, Conversion of above- and below-bandgap photons via InAs quantum dot media embedded into GaAs solar cell, Appl. Phys. Lett. 104 (2014) 253904.
[76] A. Luque, A. Martí, Increasing the efficiency of ideal solar cells by photon induced transitions at intermediate levels, Phys. Rev. Lett. 78 (1997) 5014.
[77] P. Lam, J. Wu, M. Tang, D. Kim, S. Hatch, I. Ramiro, et al., InAs/InGaP quantum dot solar cells with an AlGaAs interlayer, Sol. Energy Mater. Sol. Cell 144 (2016) 96–101.
[78] E.H. Sargent, Colloidal quantum dot solar cells, Nat. Photon. 6 (2012) 133–135.
[79] G.H. Carey, A.L. Abdelhady, Z. Ning, S.M. Thon, O.M. Bakr, E.H. Sargent, Colloidal quantum dot solar cells, Chem. Rev. (2015).
[80] A.J. Nozik, M.C. Beard, J.M. Luther, M. Law, R.J. Ellingson, J.C. Johnson, Semiconductor quantum dots and quantum dot arrays and applications of multiple exciton generation to third-generation photovoltaic solar cells, Chem. Rev. 110 (2010) 6873–6890.
[81] Z. Ning, X. Gong, R. Comin, G. Walters, F. Fan, O. Voznyy, et al., Quantum-dot-in-perovskite solids, Nature 523 (2015) 324–328.
[82] J. Zhou, Y. Yang, Zhang C-y: toward biocompatible semiconductor quantum dots: from biosynthesis and bioconjugation to biomedical application, Chem. Rev. 115 (2015) 11669–11717.
[83] X. He, N. Ma, An overview of recent advances in quantum dots for biomedical applications, Colloid Surface B 124 (2014) 118–131.
[84] B.A. Kairdolf, A.M. Smith, T.H. Stokes, M.D. Wang, A.N. Young, S. Nie, Semiconductor quantum dots for bioimaging and biodiagnostic applications, Annu. Rev. Anal. Chem. 6 (2013) 143.
[85] R. Cui, H.-H. Liu, H.-Y. Xie, Z.-L. Zhang, Y.-R. Yang, D.-W. Pang, et al., Living yeast cells as a controllable biosynthesizer for fluorescent quantum dots, Adv. Funct. Mater. 19 (2009) 2359–2364.
[86] C. Mi, Y. Wang, J. Zhang, H. Huang, L. Xu, S. Wang, et al., Biosynthesis and characterization of CdS quantum dots in genetically engineered Escherichia coli, J. Bootechnol. 153 (2011) 125–132.
[87] S.R. Sturzenbaum, M. Hockner, A. Panneerselvam, J. Levitt, J.S. Bouillard, S. Taniguchi, et al., Biosynthesis of luminescent quantum dots in an earthworm, Nat. Nanotechnol. 8 (2013) 57–60.
[88] A. Valizadeh, H. Mikaeili, M. Samiei, S.M. Farkhani, N. Zarghami, A. Akbarzadeh, et al., Quantum dots: synthesis, bioapplications, and toxicity, Nanoscale Res. Lett. 7 (2012) 1–14.
[89] I. Schick, S. Lorenz, D. Gehrig, S. Tenzer, W. Storck, K. Fischer, et al., Inorganic Janus particles for biomedical applications, Beilstein J. Nanotechnol. 5 (2014) 2346–2362.
[90] A. Walther, A.H.E. Müller, Janus particles: synthesis, self-assembly, physical properties, and applications, Chem. Rev. 113 (2013) 5194–5261.
[91] S.N. Yin, C.F. Wang, Z.Y. Yu, J. Wang, S.S. Liu, S. Chen, Versatile bifunctional magnetic-fluorescent responsive janus supraballs towards the flexible bead display, Adv. Mater. 23 (2011) 2915–2919.
[92] M. Yoshida, K.H. Roh, S. Mandal, S. Bhaskar, D. Lim, H. Nandivada, et al., Structurally controlled bio-hybrid materials based on unidirectional association of anisotropic microparticles with human endothelial cells, Adv. Mater. 21 (2009) 4920–4925.